Eur. Phys. J. B **56**, 247–252 (2007)
DOI: 10.1140/epjb/e2007-00116-5

THE EUROPEAN
PHYSICAL JOURNAL B

Multi-value cellular automata model for mixed bicycle flow

B. Jia[1,a], X.-G. Li[1,2], R. Jiang[3], and Z.-Y. Gao[1,2]

[1] School of Traffic and Transportation, Beijing Jiaotong University, Beijing 100044, P.R. China
[2] State Key Laboratory of Railway Traffic Control and Safety, Beijing Jiaotong University, Beijing 100044, P.R. China
[3] School of Engineering Science, University of Science and Technology of China, Hefei 230026, P.R. China

Received 8 December 2006 / Received in final form 29 January 2007
Published online 4 May 2007 –

Abstract. In this paper, we investigate mixed bicycle flow using the multi-value cellular automata (CA) model. Two types of bicycles with different maximum speed are considered in the system. The system of mixed bicycles is investigated under both deterministic and stochastic regimes. It is shown under the deterministic case that there appear multiple states both in congested flow and free flow regions. Analytical analysis is carried out and is in good agreement with the simulation results. Under the stochastic case, the multiple states effect disappears only when both slow and fast bicycles are randomized. Spacetime plots are presented to show the evolution of mixed bicycle flow.

PACS. 05.50.+q Lattice theory and statistics – 02.50.Ey Stochastic processes – 64.75.+g Solubility, segregation, and mixing – 89.90+n Other topics in areas of applied and interdisciplinary physics

1 Introduction

Traffic problems have attracted much attention in recent decades [1–3]. Traffic flow is a kind of many-body system of strongly interacting vehicles, and it can exhibit very complex behavior. Many theoretical models have been proposed to explore the mechanisms in traffic flow [4–9]. Among them we will focus on Cellular automata (CA) models. CA has become an efficient tool for simulating traffic flow, for it is conceptually simple and can be easily implemented on computers for numerical investigations.

The rule-184 [10] CA is a prototype of all CA models for traffic flow. In 1992, Nagel and Schreckenberg proposed the well-known Nagel-Schreckenberg (NS) model [7]. As an extension of rule-184 CA, higher speeds are allowed in the NS model. The NS model can reproduce some basic phenomena encountered in real traffic, such as spontaneous jams. However, it cannot explain such empirically observed phenomena as metastable states, capacity drop and synchronized flow. Therefore, several improved versions of the NS model were proposed, such as the anticipation model [8], the slow-to-start model [9], etc.

Recently, Nishinari and Takahashi proposed a family of multi-value CA models [11–13]. Different from previous cases, in these models each site is assumed to hold L vehicles at most. The basic version of the family is obtained from an ultradiscretization of the Burgers equation, so it is called the Burger cellular automata (BCA). Its evolution equation is

$$U_j(t+1) = U_j(t) + \min(U_{j-1}(t), L - U_j(t)) - \min(U_j(t), L - U_{j+1}(t)) \quad (1)$$

where $U_j(t)$ represents the number of vehicles at site j and time t. If it is assumed that the road is an L-lane freeway, then the model can describe the multi-value traffic without explicitly considering the lane-changing rule.

The maximum velocity of vehicles in BCA is 1. Nishinari and Takahashi have extended BCA for the case of maximum velocity 2 and presented extended BCA (EBCA) models [13]. Matsukidaira and Nishinari have investigated the Euler-Lagrange correspondence of cellular automata models for traffic flow [14,15] and proposed the generalized BCA (GBCA) model with high speed and long perspective [16]. In our previous work [17], the EBCA models were used to model bicycle flow, and stochastic randomization was introduced into the models.

In real traffic, bicycles do not have the same maximum velocity due to differences in the personalities of riders. For example, young riders always tend to ride at high speed, while old riders usually ride at low speed.

In this work, mixed bicycle flow is investigated using the EBCA model. There are two kinds of bicycles: slow bicycles with maximum speed 1 and fast bicycles with maximum speed 2. It is found under the deterministic case that the multiple states effect occurs both in the free flow and

[a] e-mail: bjia@bjtu.edu.cn

congested flow regions. In the stochastic case, the multiple states effect disappears only when both slow bicycles and fast bicycles are randomized.

This paper is organized as follows: the model for mixed bicycle flow is proposed in Section 2. Next the simulation results are presented and analyzed in Section 3. The conclusion is given in Section 4.

2 The multi-value CA model for mixed bicycle flow

In the EBCA model[1], bicycle movement from t to $t+1$ consists of the following two successive procedures:

(a) bicycles move to their next site if the site is not fully occupied;
(b) only bicycles which moved in procedure (a) can move a further one site if their next site is not fully occupied after procedure (a).

Therefore, the evolution equation of the EBCA is given by:

$$U_j(t+1) = U_j(t) + b_{j-1}(t) - b_j(t) + c_{j-2}(t) - c_{j-1}(t). \quad (2)$$

Here $b_j(t) = \min(U_j(t), L - U_{j+1}(t))$ represents the number of moving bicycles at site j and time t in procedure (a); $c_j(t) = \min(b_j(t), L - U_{j+2}(t) - b_{j+1}(t) + b_{j+2}(t))$ represents the number of bicycles that can move in procedure (b).

To investigate mixed bicycle flow, two kinds of bicycles, slow bicycles with maximum speed 1 and fast bicycles with maximum speed 2, are considered in the system. The number of slow bicycles and fast bicycles at site j and time t are $U_j^s(t)$ and $U_j^f(t)$ respectively. The updating procedures are changed to:

(1) all bicycles move to their next site if the site is not fully occupied, and the fast bicycles have priority over slow bicycles;
(2) only the fast bicycles moved in procedure (1) can move a further one site if their next site is not fully occupied after procedure (1).

The number of fast and slow bicycles that move one site at site j and time t in procedure (1) are $b_j^f(t)$ and $b_j^s(t)$ respectively. $c_j(t)$ represents the number of fast bicycles that move two sites at site j and time t. The randomization effect of slow bicycles is introduced as: $b_j^s(t+1)$ decreases by 1 with probability p_s if $b_j^s(t+1) > 0$. The randomization effect of fast bicycles is: $c_j(t+1)$ decreases by 1 with probability p_f if $c_j(t+1) > 0$. The updating rules are as follows:

Step 1: calculation of $b_j^f(t+1)$, $b_j^s(t+1)$ and $b_j(t+1)$ $(j = 1, 2, \ldots, K)$:
$b_j^f(t+1) = \min(U_j^f(t), L - U_{j+1}(t))$;
$b_j^s(t+1) = \min(U_j^s(t), L - U_{j+1}(t) - b_j^f(t+1))$,
if $rand() < p_s$, $b_j^s(t+1) = \max(b_j^s(t+1) - 1, 0)$;
$b_j(t+1) = b_j^f(t+1) + b_j^s(t+1)$.
$b_j^f(t+1)$ is calculated first because the fast bicycles have priority over slow bicycles.

Step 2: calculation of $c_j(t+1)$:
$$c_j(t+1) = \min(b_j^f(t+1), L - U_{j+2}(t) - b_{j+1}(t+1) + b_{j+2}(t+1));$$
if $rand() < p_f$, then
$c_j(t+1) = \max(c_j(t+1) - 1, 0)$.

Step 3: updating $U_j(t+1)$, $U_j^s(t+1)$ and $U_j^f(t+1)$:
$$U_j^f(t+1) = U_j^f(t) - b_j^f(t+1) + b_{j-1}^f(t+1) - c_{j-1}(t+1) + c_{j-2}(t+1);$$
$$U_j^s(t+1) = U_j^s(t) - b_j^s(t+1) + b_{j-1}^s(t+1);$$
$$U_j(t+1) = U_j^f(t+1) + U_j^s(t+1).$$

Here $rand()$ is an uniformly distributed random number between 0 and 1.

[1] Here we consider only the EBCA1 model, the extension of the EBCA2 model to mixed bicycle flow will be carried out in a future study.

3 Simulation results

In the simulations, $L = 4$ and $K = 100$ are selected where K is the length of the road. Periodic conditions are used so the bicycles ride on a circuit. In the initial state, slow bicycles and fast bicycles are randomly distributed on the road. The proportion of slow bicycles is R. The number of fast (slow) bicycles in the system is $N_f = (1 - R)\rho LK$ ($N_s = R\rho LK$). We note that the new model with $R = 0.0$ is equivalent to the stochastic EBCA1 model, and that with $R = 1.0$ corresponds to the stochastic BCA model. The average density ρ and flow Q over all sites are defined by

$$\rho = \frac{1}{KL}\sum_{j=1}^{K} U_j(t) \quad Q(t) = \frac{1}{KL}\sum_{j=1}^{K}(b_{j-1}(t) + c_{j-2}(t)). \quad (3)$$

3.1 Deterministic case

In this subsection, we focus on the deterministic case, i.e., $p_s = 0.0$ and $p_f = 0.0$. The fundamental diagrams are shown in Figure 1. In the case of $R = 0.0$, the multiple states effect is observed only in the congested flow region (Fig. 1a). In other words, there is only one branch with positive slope but there are several branches with negative slope. The detailed analysis of the multiple states has been given in reference [13].

When $0 < R < 1$, one finds that the multiple states effect occurs both in the congested flow and free flow regions, i.e., there are several branches with positive slope as well as several branches with negative slope. With increasing R, the number of branches with positive slope decreases. Simultaneously, the multiple states effect in the congested flow region is also suppressed. When $R = 1$, the multiple states effect disappears.

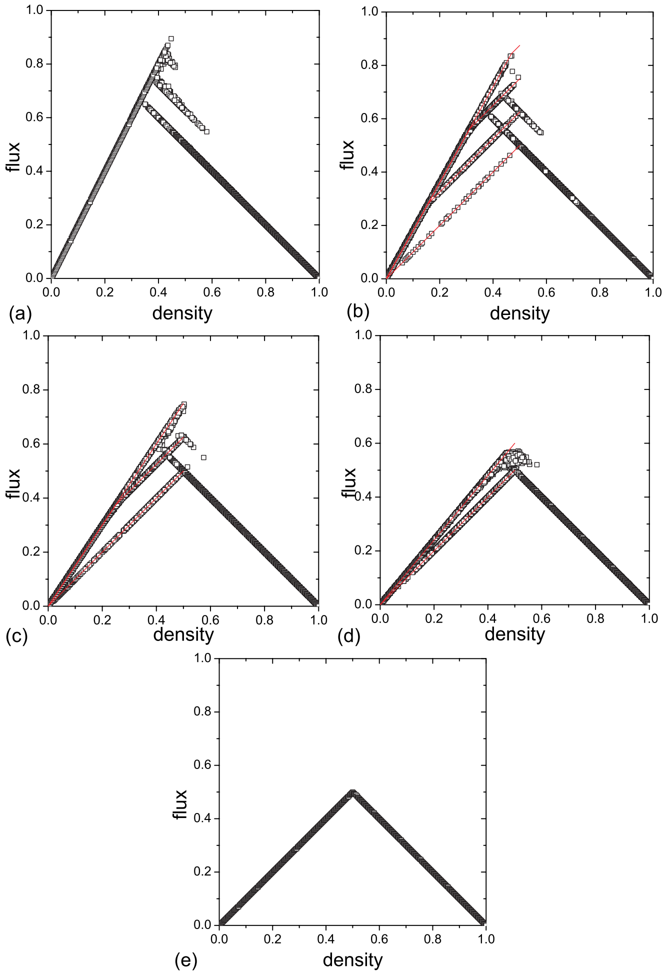

Fig. 1. The fundamental diagrams in the case of (a) $R = 0.0$ (b) $R = 0.2$ (c) $R = 0.5$ (d) $R = 0.8$ (e) $R = 1.0$. The red lines correspond to the analytical values.

Next we focus on the branches with positive slope. Our simulations show that in the free flow region, every slow bicycle can move in each time step. Therefore, the average velocity of the system is given by

$$\bar{v} = \frac{N_s \times 1 + N_f \times \bar{v}_f}{N_s + N_f}.$$

Here N_s and N_f are the number of slow and fast bicycles respectively; $\bar{v}_f$ is the average velocity of the fast bicycles. Since $L = 4$ is used in the simulations, next four subcases are classified:

1. There exist four slow bicycles that occupy one site. In this case, these four slow bicycles form a moving bottleneck by moving side by side. Fast bicycles cannot overtake them and have to follow behind them. As a result, $\bar{v}_f = 1$ and $\bar{v} = 1$. The flow rate is, therefore, $Q = \rho$. This gives the lowest free flow branch in Figures 1b–1e.
2. There exist at most three slow bicycles at each site. In this case, there will be one fast bicycle overtaking the moving bottleneck formed by the three slow bicycles at each time step. Due to the parallel update rule, this allows at most $K/2$ fast bicycles to move with velocity 2. As a result,

$$\bar{v}_f = \frac{(N_f - K/2) \times 1 + K/2 \times 2}{N_f} \text{ for } N_f > K/2$$

and

$$\bar{v}_f = 2 \text{ for } N_f \leq K/2.$$

Therefore, the flow rate is

$$Q = \rho \left[\frac{N_s \times 1 + N_f \times 2}{N_s + N_f}\right] \text{ for } N_f \leq K/2 \quad (4)$$

and

$$Q = \rho \left[\frac{N_s \times 1 + N_f \times \frac{(N_f - K/2) \times 1 + K/2 \times 2}{N_f}}{N_s + N_f}\right] \text{ for } N_f > K/2. \quad (5)$$

Substituting $N_s = \rho KLR$ and $N_f = \rho KL(1 - R)$ into equations (4) and (5), one has

$$Q = \rho(2 - R) \text{ for } \rho \leq \frac{1}{2L(1 - R)} \quad (6)$$

and

$$Q = \rho + \frac{1}{2L} \text{ for } \rho > \frac{1}{2L(1 - R)}. \quad (7)$$

Equation (7) gives the second lowest free flow branch in Figures 1b and 1c, and equation (6) gives the high free flow branch in Figure 1d.

3. There exist at most two slow bicycles at each site. In this case, there will be two fast bicycle overtaking the two slow bicycles each time step. This allows at most $K/2 \times 2 = K$ fast bicycles to move with velocity 2. Similarly to case 2, we have

$$Q = \rho(2 - R) \text{ for } \rho \leq \frac{1}{L(1 - R)} \quad (8)$$

and

$$Q = \rho + \frac{1}{L} \text{ for } \rho > \frac{1}{L(1 - R)}. \quad (9)$$

Equation (9) gives the second highest free flow branch in Figure 1b, and equation (8) gives the high free flow branch in Figure 1c.

4. There exists at most one slow bicycle in each site. Similarly to cases 2 and 3, we have

$$Q = \rho(2 - R) \text{ for } \rho \leq \frac{3}{2L(1 - R)} \quad (10)$$

and

$$Q = \rho + \frac{3}{2L} \text{ for } \rho > \frac{3}{2L(1 - R)}. \quad (11)$$

Equation (10) gives the highest free flow branch in Figure 1b. The states determined by equation (11) are unstable and will transit into congested states.

Fig. 2. Spacetime plots of the deterministic case when $R = 0.5, \rho = 0.4$. (a) (c) and (e) show the number of slow bicycles in each site, while (b) (d) and (f) show the number of fast bicycles in each site. The bicycles move from left to right, and the vertical direction (down) is (increasing) time. (a) and (b) in low branch; (c) and (d) in mid branch; (e) and (f) in upper branch.

From Figure 1, we can see that the simulation results are consistent with the analytical results, except that some high flux states are not reached in the simulation. In real bicycle flow, a group of cyclists may ride together because that they are class mates, friends or colleagues. They will occupy a large part of the cycle lane, thus the bicycles that follow are blocked. We argue that the multiple states effect in the free flow region surely occurs in real bicycle flow.

Next some spacetime structures of the mixed bicycle flow are investigated to illustrate the above analytical results. We choose the parameters $R = 0.5$ and $\rho = 0.4$. There are three flow rates corresponding to the density: $Q_{low} = 0.4$, $Q_{mid} = 0.525$ and $Q_{up} = 0.6$. In the low branch (Figs. 2a and 2b), there exist four slow bicycles moving side by side. The fast bicycles cannot overtake these four bicycles and assemble behind them. As a result, the fast bicycles and the slow bicycles are well separated. In the mid branch (Figs. 2c and 2d), there exist at most three slow bicycles in each site. As a result, only one fast bicycle can overtake these three bicycles in each time step.

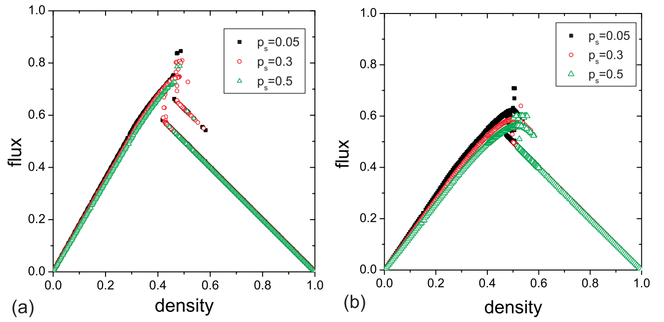

Fig. 3. The fundamental diagrams with different values of p_s when $p_f = 0.0$. (a) $R = 0.2$ and (b) $R = 0.5$.

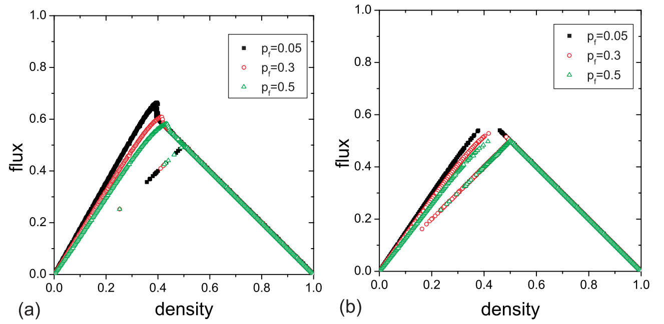

Fig. 4. The fundamental diagrams with different values of p_f when $p_s = 0.0$. (a) $R = 0.2$ and (b) $R = 0.5$.

Thus, fast bicycles form a steady state "$\cdots 01010101 \cdots$" downstream of the three slow bicycles. In the up branch (Figs. 2e and 2f), there exist at most two slow bicycles in each site, and both the slow bicycles and the fast bicycles are moving with free flow speed because $N_f \leq K/2 \times 2$.

3.2 Stochastic case

In this subsection, we investigate the effect of randomization in the mixed bicycle flow. To this end, two typical values of R are chosen: $R = 0.2$ and $R = 0.5$.

Firstly we consider the case $p_f = 0$ and $p_s > 0$. From Figure 3, one can see the multiple states effect does not occur in the free flow region but still exists in the congested region. This is because with the consideration of the randomization effect of slow bicycles, a stationary moving bottleneck will not exist. A large moving bottleneck may split into several small ones and several small moving bottlenecks may merge into one large one. This breaks the mechanism of multiple branches shown in the previous subsection.

The fundamental diagram only slightly depends on the value of p_s when the ratio of slow bicycles is small (Fig. 3a). However, when the ratio of slow bicycles increases, the maximum flow rate notably decreases with the increase of p_s (Fig. 3b).

Next we consider the case $p_f > 0$ and $p_s = 0$. Figure 4 shows the multiple states effect does not occur in the congested flow region. However, there always exists two branches in the free flow region. The branch $Q = \rho$

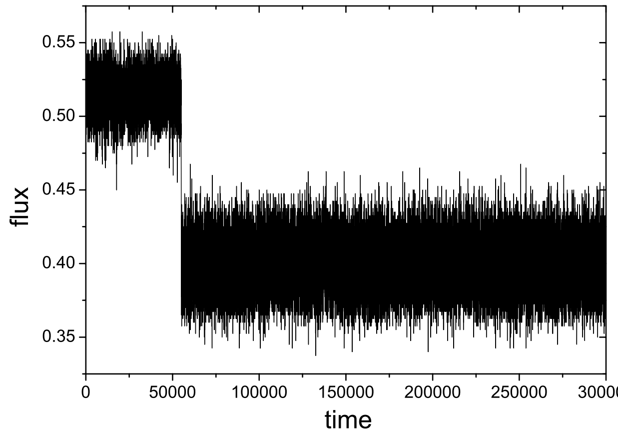

Fig. 5. Time evolution of the flux at $\rho = 0.4$ in the case of $R = 0.5$. The parameters are $p_s = 0.0$ and $p_f = 0.3$. Note that the duration of large flow rate depends on the initial condition and the system size K.

(the low branch) exists because once four slow bicycles appear in one site, this moving bottleneck will not dissolve since no randomization is exerted on slow bicycles. The high branch exists in the situations that four slow bicycles never appear in one site. When the ratio of slow vehicles is small, the chance that four slow bicycles appear in one site is small. As a result, the data points on the low branch are sparse (Fig. 4a).

The value of p_f only affects the high branch. As p_f increases, the flux in the free flow region decreases. We also note that there is a gap between the high branch and the congested branch in the case of $R = 0.5$. This is because in the intermediate range of density, the appearance of four slow bicycles in one site will always occur sooner or later. For example, see Figures 5 and 6. Initially there are not four bicycles occupying one site. As a result, a large flow rate is maintained. After some evolution time, four slow bicycles accumulate on one site. This moving bottleneck will not dissolve and it hinders the movement of fast bicycles. Consequently, a flow rate drop appears.

In contrast, the probability that four slow bicycles appear in one site is small in the intermediate range of density in the case of $R = 0.2$. Therefore, there is not a gap between the high branch and the congested branch.

Figures 7a and 7b show the results with randomization parameter $p_s > 0$ and $p_f > 0$. One can see that the multiple states effect disappears even if p_s and p_f are slightly larger than zero. As p_s and p_f increase, the maximum flow rate decreases and the density corresponding to the maximum flow rate increases.

Finally, we would like to point out the properties of mixed bicycle flow are different from that of mixed vehicle flow. In mixed vehicle flow, the flux is constrained by the plug formed by slow vehicles [18,19]. The fundamental diagram will be essentially the same as in the case of $R = 1.0$ even if only a small number of slow vehicles are introduced into the system. However, in mixed bicycle flow, introducing a small proportion of slow bicycles will

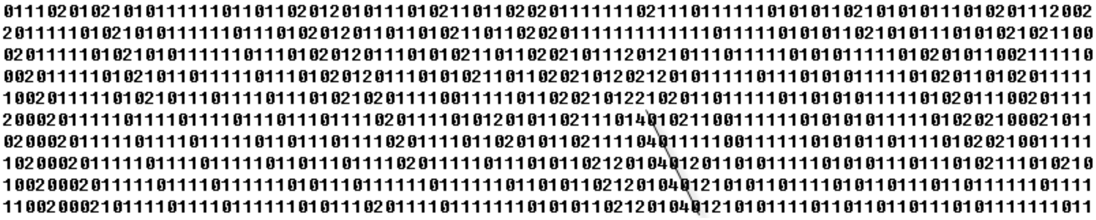

Fig. 6. The spacetime plot of the number of slow bicycles in each site around the transition from high flux to low flux in Figure 5. The formation of a 4-lane blockage is marked with a line.

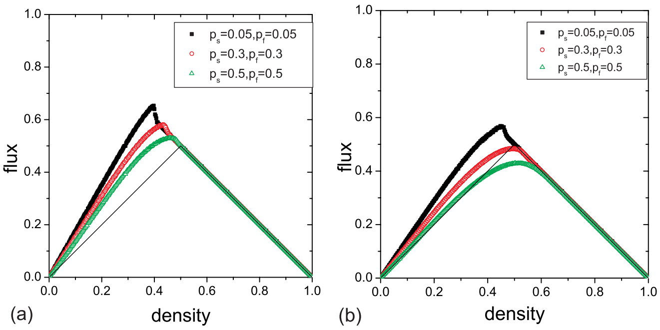

Fig. 7. The fundamental diagrams with different values of p_s and p_f. (a) $R = 0.2$ and (b) $R = 0.5$. The solid line corresponds to the case of $R = 1.0$ with $p_s = 0.0$.

not affect the flow rate so much. This can be seen from Figure 7, in which the flow rate in the case of $R = 0.2$ is significantly larger than in the case of $R = 1.0$. We believe this difference is mainly because the bicycle lanes are not so clearly separated from each other as vehicle lanes.

4 Conclusion

In this paper, mixed bicycle flow is investigated using the multi-value CA model. Both the deterministic and the stochastic case are studied. The fundamental diagrams and the spacetime plots are analyzed in detail.

In the deterministic case, the multiple states effect exists both in the free flow and congested regions. The site which contains the largest number of slow bicycles forms a moving bottleneck to the system and the flux is constrained by this bottleneck. The simulation results are consistent with the analytical ones.

In the stochastic case, the multiple states effect disappears in the free flow region when $p_s > 0.0$, and it disappears in the congested region when $p_f > 0.0$. The multiple states effect disappears when both slow bicycles and fast bicycles are randomized.

In our future work, we will extend the EBCA2 model to study mixed bicycle flow and compare the results of the two models. The calibration and verification of the models using real bicycle flow data will also be performed.

This work is partially supported by the National Basic Research Program of China under No. 2006CB705500, the National Natural Science Foundation of China under Key Project Nos. 70631001, 10532060 and Project Nos. 70501004, 70471088 and 10404025, Special Program for the Preliminary Research of the Momentous Fundamental Research under No. 2005CCA03900, and the Science and Technology Foundation of Beijing Jiaotong University under No. 2004SM026.

References

1. D. Chowdhury, L. Santen, A. Schadschneider, Physics Reports **329**, 199 (2000)
2. D. Helbing, Rev. Mod. Phys. **73**, 1067 (2001)
3. T. Nagatani, Rep. Prog. Phys. **65**, 1331 (2002)
4. M. Bando, K. Hasebe, A. Nakayama, A. Shibata, Y. Sugiyama, Phys. Rev. E **51**, 1035 (1995)
5. H.Y. Lee, H.W. Lee, D. Kim, Phys. Rev. Lett. **81**, 1130 (1998)
6. B.S. Kerner, S.L. Klenov, D.E. Wolf, J. Phys. A: Math. Gen. **35**, 9971 (2002)
7. K. Nagel, M. Schreckenberg, J. Physique I **2**, 2221 (1992)
8. X.B. Li, Q.S. Wu, R. Jiang, Phys. Rev. E **64**, 066128 (2001)
9. S.C. Benjamin, N.F. Johnson, P.M. Hui, J. Phys. A: Math. Gen. **29**, 3119 (1996); R. Barlovic, L. Santen, A. Schadschneider et al., Eur. Phys. J. B **5**, 793 (1998)
10. S. Wolfram, *Theory and Applications of Cellular Automata* (World Scientific, Singapore, 1986)
11. K. Nishinari, D. Takahashi, J. Phys. A: Math. Gen. **31**, 5439 (1998)
12. K. Nishinari, D. Takahashi, J. Phys. A: Math. Gen. **32**, 93 (1999)
13. K. Nishinari, D. Takahashi, J. Phys. A: Math. Gen. **33**, 7709 (2000)
14. K. Nishinari, J. Phys. A: Math. Gen. **34**, 10727 (2001)
15. J. Matsukidaira, K. Nishinari, Phys. Rev. Lett. **90**, 088701 (2003)
16. J. Matsukidaira, K. Nishinari, Int. J. Mod. Phys. C **15**, 507 (2004)
17. R. Jiang, B. Jia, Q.S. Wu, J. Phys. A: Math. Gen. **37**, 2063 (2004)
18. D. Chowdhury, D.E. Wolf, M. Schreckenberg, Physica A **235**, 417 (1997)
19. W. Knospe, L. Santen, A. Schadschneider, M. Schreckenberg, Physica A **265**, 614 (1999)